J Mater Sci (2010) 45:593–598
DOI 10.1007/s10853-009-3932-7

Gadolinium-doped cerium oxide nanorods: novel active catalysts for ethanol reforming

Mario Godinho · Rosana de F. Gonçalves · Edson R. Leite · Cristiane W. Raubach · Neftalí L. V. Carreño · Luiz F. D. Probst · Elson Longo · Humberto V. Fajardo

Received: 7 April 2009 / Accepted: 28 September 2009 / Published online: 10 October 2009

Abstract The gadolinium-doped ceria nanorods ($Gd_{0.2}Ce_{0.8}O_{2-x}$) were synthesized by hydrothermal treatment. It was shown that the use of microwave heating during hydrothermal treatment decreases the treatment time required to obtain gadolinium-doped ceria nanorods and that oriented attachment is the dominant mechanism responsible for anisotropic growth. It was clear that $Gd_{0.2}Ce_{0.8}O_{2-x}$ nanorods were more catalytically active than commercial CeO_2 in the ethanol reforming reaction.

M. Godinho
Centro Universitário do Leste de Minas Gerais, 35170-056 Coronel Fabriciano, MG, Brazil

R. de F. Gonçalves · E. R. Leite
Departamento de Química, Universidade Federal de São Carlos, 13565-905 São Carlos, SP, Brazil

C. W. Raubach · N. L. V. Carreño
Departamento de Química Analítica e Inorgânica, Universidade Federal de Pelotas, 96010-900 Capão do Leão, RS, Brazil

L. F. D. Probst
Departamento de Química, Universidade Federal de Santa Catarina, 88040-900 Florianópolis, SC, Brazil

E. Longo
Departamento de Bioquímica e Tecnologia Química, Universidade Estadual Paulista, 15385-000 Araraquara, SP, Brazil

H. V. Fajardo (✉)
Departamento de Química, Instituto de Ciências Exatas e Biológicas, Campus Universitário s/n Bauxita, Universidade Federal de Ouro Preto, 35400-000 Ouro Preto, MG, Brazil
e-mail: hfajardo@iceb.ufop.br

Introduction

Cerium oxide has been extensively studied due to its commercial applications as a catalyst, oxygen sensor, solid electrolyte, and absorbent, among others. It is well known that cerium oxide is used as a catalyst in a wide variety of reactions of industrial and environmental interest. This oxide has a high oxygen mobility and storage capacity, and can act as a local source or sink for oxygen involved in reactions taking place on its surface. In spite of these interesting characteristics, the major limitation to applying CeO_2 as a catalyst is its low specific surface area and poor textural stability under certain reduction conditions [1–3]. However, numerous techniques have been proposed to synthesize nanosized CeO_2-based materials with promising control of the properties [3–9]. In recent years, ceria and ceria-doped anisotropic nanocrystals, particularly nanorods, have been obtained through several solution-based synthetic routes, with special attention focusing on routes based on the precipitation and aging of the precipitate under hydrothermal conditions. The main reason for this interest in ceria-based anisotropic nanocrystals is the possibility of developing catalytic materials with high surface area and well-defined reactive crystal planes with superior catalytic activity. In addition, the performance of nanometric CeO_2 in some catalytic processes can be improved depending on the shape [9, 10]. Therefore, the objective of this study was to present the synthesis and characterization of gadolinium-doped cerium oxide nanorods as a novel and active catalyst to promote the ethanol reforming reaction. Nowadays, with the shortage of natural resources and energy, and also the skyrocketing prices of crude oil, the production of valuable products, such as hydrogen and ethylene, from nonpetroleum, environment friendly, raw materials presents a challenge to researchers in this area. Bioethanol is an attractive

alternative feedstock for use in the production of these chemicals [11–13].

Experimental

Sample preparation

Gadolinium-doped ceria nanorods, with a nominal composition of $Gd_{0.2}Ce_{0.8}O_{2-x}$, were synthesized by hydrothermal treatment of a colloidal suspension of gadolinium-doped ceria nanocrystals in an aqueous solution. First, 0.1 mol/L of hexahydrated cerium(III) nitrate ($Ce(NO_3)_3 \cdot 6H_2O$, Aldrich) was dissolved in high purity water in polytetrafluoroethylene vessels. After complete dissolution of the cerium nitrate, gadolinium(III) oxide (Gd_2O_3, Aldrich) dissolved in a minimal amount of nitric acid was added to the solution. Under magnetic stirring, ammonium hydroxide (0.1 mol/L) was added dropwise to complete the precipitation (final pH = 10), resulting in a white gel. The polytetrafluoroethylene vessels containing the gadolinium-doped ceria nanocrystals were then treated under a hydrothermal condition (130 °C, 3 atm pressure, for 30 min). The hydrothermal treatment was carried out in a microwave oven. After the hydrothermal treatment, the powder in suspension was centrifuged and washed in distilled water until the residual ions in the solution were completely eliminated. The resulting product was dried at room temperature for 48 h.

Sample characterization

The structural analysis of gadolinium-doped ceria nanorods was carried out by X-ray diffraction (XRD) (Rigaku D-Max 2500) using CuK_α radiation and a graphite monochromator.

The structure and morphology of the samples were verified by transmission electron microscopy (TEM), and high-resolution transmission electron microscopy (HR-TEM) (Jeol, model 3010, operated at 300 KV) equipped with X-ray energy dispersive spectroscopy.

Samples were characterized by N_2 adsorption/desorption isotherms obtained at the temperature of liquid nitrogen using an automated physisorption instrument (Autosorb-1C, Quantachrome Instruments). Specific surface areas were calculated according to the Brunauer–Emmett–Teller (BET) method and the pore size distributions were obtained according to the Barret–Joyner–Halenda (BJH) method from the adsorption data.

Catalytic tests

Catalytic performance tests were conducted at atmospheric pressure with a quartz fixed-bed reactor fitted in a programmable oven, at temperatures of 400, 500, and 600 °C. The reaction mixture (water:ethanol, molar ratio 3:1) was pumped into a heated chamber and vaporized. The water–ethanol gas (N_2) stream (30 mL/min) was then fed to the reactor containing 250 mg of the catalyst. The catalysts ($Gd_{0.2}Ce_{0.8}O_{2-x}$ nanorods and commercial CeO_2, Riedel-de Haën) were previously treated in situ under nitrogen atmosphere at 500 °C for 2 h. The reactants and the composition of the reactor effluent were analyzed with a gas chromatograph (Shimadzu GC 8A), equipped with a thermal conductivity detector, a Porapak-Q and a 5A molecular sieve column with Ar as the carrier gas. Reaction data were recorded during 4 h.

Results and discussion

Sample characterizations

The specific surface area measurements (Table 1) show that the $Gd_{0.2}Ce_{0.8}O_{2-x}$ nanorods have a higher specific surface area and pore volume compared to the commercial CeO_2, with respective values of 29 m^2/g and 0.031 cm^3/g. Figure 1 shows the XRD pattern of the synthesized materials before and after hydrothermal treatment in a microwave oven. Before the treatment, one can observe the pattern of a crystalline material indicating the formation of a single phase with a cubic fluorite structure composed of broad peaks typical of nanocrystalline materials. The crystallite size, calculated from the XRD data and Scherrer's equation was 3.1 nm. After the hydrothermal treatment, the material preserved the fluorite structure with a well-defined XRD pattern with narrow peaks, suggesting that no phase transformation occurred during the treatment. Figure 2a, b shows the bright-field (BF) TEM images of the material after hydrothermal treatment in a microwave oven, indicating the presence of gadolinium-doped ceria nanorods. The nanorods had lengths of 50–500 nm and diameters of 20–60 nm. The synthesized gadolinium-doped ceria nanorods showed a morphology similar to that reported by Zhou et al. [9] and Mai et al. [10]. However, these studies used traditional heating techniques and longer treatment times. In the present study, the use of microwave

Table 1 N_2 physisorption characterization

Catalysts	S_{BET}[a]	V_{BJH}[b]
$Ce_{0.8}Gd_{0.2}O_2$ nanorods	29	0.031
Commercial CeO_2	5	0.004

Specific surface area and pore volume of gadolinium-doped cerium oxide and commercial cerium oxide catalysts

[a] Specific surface area—m^2/g, BET method

[b] Pore volume—cm^3/g, BJH method

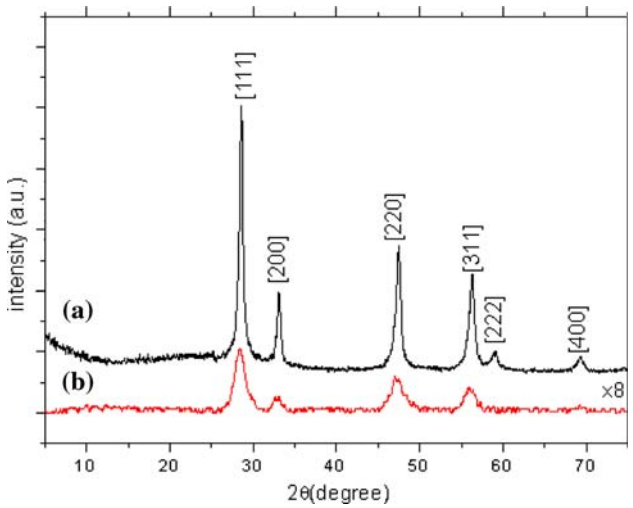

Fig. 1 XRD pattern of the material before (*a*) and after (*b*) hydrothermal treatment in a microwave oven

heating allowed for a shorter treatment time (30 min). In a previous study [14], we found that a controlled experiment, performed under hydrothermal conditions using a traditional heating technique (electric oven) and similar experimental parameters (temperature, time, composition, and pressure), did not indicate the formation of gadolinium-doped ceria nanorods. The only formation observed was gadolinium-doped ceria nanocrystals with particle sizes of 10–15 nm, clearly indicating that microwave heating accelerates the formation of nanorods. A closer examination of the BF-TEM image in Fig. 2b reveals that the $Gd_{0.2}Ce_{0.8}O_{2-x}$ nanorods are composed of several nanoparticles, as indicated by the arrows. This finding offers important information and can shed light on the crystal growth mechanism. The HR-TEM characterization of the material after hydrothermal treatment presented interesting results concerning the nanorods formation mechanism. The HR-TEM images in Fig. 3a–c confirm that the anisotropic particles were composed of several primary particles. In fact, the HR-TEM image reveals that the nanorods were composed of oriented primary particles, as indicated by the arrows in Fig. 3a and by the additional

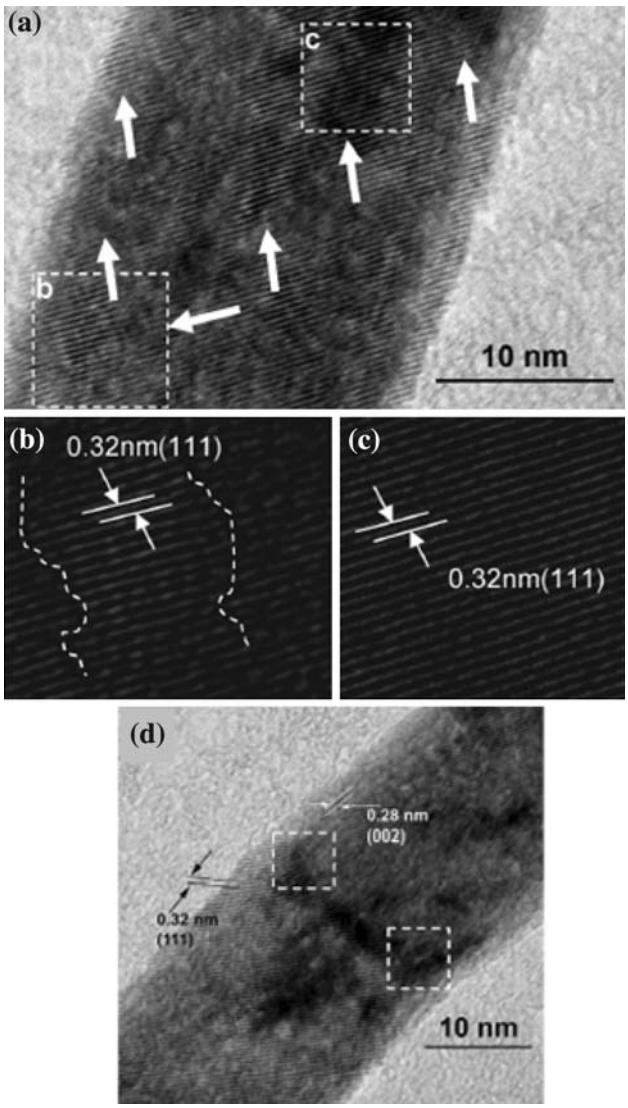

Fig. 3 **a**, **d** HR-TEM images of the material after hydrothermal treatment in a microwave oven; **b**, **c** reconstructed lattice images of different areas (indicated in panel **a**)

images in Fig. 3b, c. Figure 3b, c shows the reconstructed lattice images of different areas, showing the boundaries between the particles (indicated by the dashed white line in

Fig. 2 TEM images of the material after hydrothermal treatment in a microwave oven

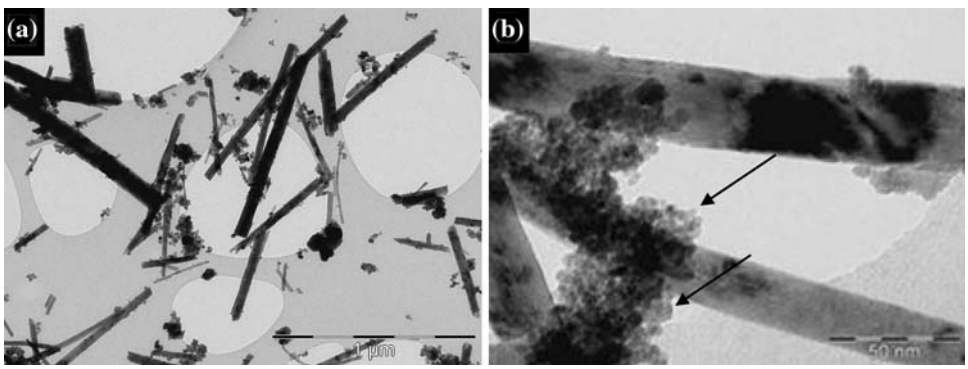

Fig. 3b) and a region with perfect attachment and alignment between particles, without defects (Fig. 3c). Figure 3d shows an interesting HR-TEM image of a nanorod with an imperfect attachment. The imperfectly oriented attachment may produce different kinds of defects. The aggregation of several nanocrystals with similar crystallographic orientations originating a single nanorod, as well as the presence of defects, is strong evidence that the orientated attachment process is the predominant nanocrystal growth mechanism during the formation of $Gd_{0.2}Ce_{0.8}O_{2-x}$ nanorods. The HR-TEM results revealed that the diameter dimensions of the nanorods were related to the (002) direction of the lattice. We also observed the lattice direction (111). This crystallographic information indicates the formation of nanorods with preferential growth in the direction [110]. This growth direction is in agreement with the fact that the driving force for the coalescence process in the orientated attachment mechanism is related to the reduction in surface energy, which can minimize the area of high-energy faces. In a cubic system, the {111} plane is the most stable (with the lowest surface energy). Thus, growth in {110} is expected. It is important to note that no notable preferential growth is observed in the XRD pattern of the $Gd_{0.2}Ce_{0.8}O_{2-x}$ nanorod sample. This particular behavior in relation to the expected preferential growth in the [110] direction, as observed by HR-TEM, should lead to an increase in the (220) reflection. However, a close look at the TEM and HR-TEM images shows a simultaneous growth process in the [200] and [111] directions, and not only in the [110] direction. Thus, an increase in the intensity of the (200) and (111) reflections should occur, resulting in a XRD pattern with no evidence of preferential growth. The XRD analysis was also performed on a sample without purification, that is, a sample with nanorods and nanocrystals. The presence of nanocrystals can modify the intensity of the reflections, especially the (111) reflection.

The catalytic behavior of the $Gd_{0.2}Ce_{0.8}O_{2-x}$ nanorods was investigated and compared to that of the commercial CeO_2 powder. Typical experimental results were obtained, as shown in Fig. 4, in which the selectivity of each product and the conversion of ethanol are shown as a function of time. It is clear that $Gd_{0.2}Ce_{0.8}O_{2-x}$ nanorods are more active than the commercial CeO_2 catalyst. At 500 °C, the percentage of ethanol conversion was around 75% over the $Gd_{0.2}Ce_{0.8}O_{2-x}$ nanorods and 45% over the commercial catalyst. As expected, the conversion of ethanol over $Gd_{0.2}Ce_{0.8}O_{2-x}$ nanorods increased with increasing reaction temperature. The complete conversion of ethanol was achieved when the temperature was 600 °C (Fig. 4c). At a temperature of 400 °C, the conversion of ethanol reached 25% at the beginning of the test (Fig. 4a), however, the ethanol conversion decreased after 250 min in time on stream. The process at this temperature was highly selective to ethylene production, with lower amounts of hydrogen. In fact, in this time interval, significant deactivation of the catalysts was not observed. However, we believe that if the reaction had been maintained for a longer period of time we would have observed some type of catalytic deactivation, since the reaction studied produced a fair amount of ethylene, a known precursor of coke, which can lead to the deactivation of the catalyst through deposition on the surface of the material. It was observed that the steam reforming reaction of ethanol (Eq. 1) was negligible at this temperature.

$$C_2H_5OH + 3H_2O \rightarrow 6H_2 + 2CO_2 \quad (1)$$

Instead, ethanol dehydration to ethylene (Eq. 2) and an ethanol decomposition reaction (Eq. 3) seem to occur as the main reactions.

$$C_2H_5OH \rightarrow C_2H_4 + H_2O \quad (2)$$

$$C_2H_5OH \rightarrow 2H_2 + 2C + H_2O \quad (3)$$

When the temperature was increased to 500 °C, ethylene selectivity decreased, hydrogen selectivity remained relatively constant, while methane, carbon dioxide, ethane, and acetaldehyde were detected in the reaction effluent (Fig. 4b).

The presence of acetaldehyde in the reaction effluent indicates that this catalyst has a mild capability for dehydrogenation of ethanol (Eq. 4).

$$C_2H_5OH \rightarrow CH_3CHO + H_2 \quad (4)$$

Moreover, the formation of ethane was also observed, which could be formed by ethylene hydrogenation (Eq. 5).

$$C_2H_4 + H_2 \rightarrow C_2H_6 \quad (5)$$

At 600 °C, the conversion of ethanol reached 100%, remaining stable until the end of the run. It was observed that the selectivity toward ethylene, formed by ethanol dehydration, decreased to approximately 33% and methane selectivity increased considerably, suggesting that the decomposition of ethanol is favored (Eq. 6).

$$C_2H_5OH \rightarrow H_2 + CO + CH_4 \quad (6)$$

The formation of methane through the decomposition of ethanol was high and the lower CO concentration indicates that the CO formed was converted into CO_2 through the water gas shift reaction (Eq. 7) and/or possibly through CO oxidation promoted by CeO_2 (Eq. 8).

$$CO + H_2O \rightarrow CO_2 + H_2 \quad (7)$$

$$2CO + O_2 \rightarrow 2CO_2 \quad (8)$$

It is known that cerium oxide-based catalysts efficiently convert CO to CO_2 via the water gas shift reaction and can

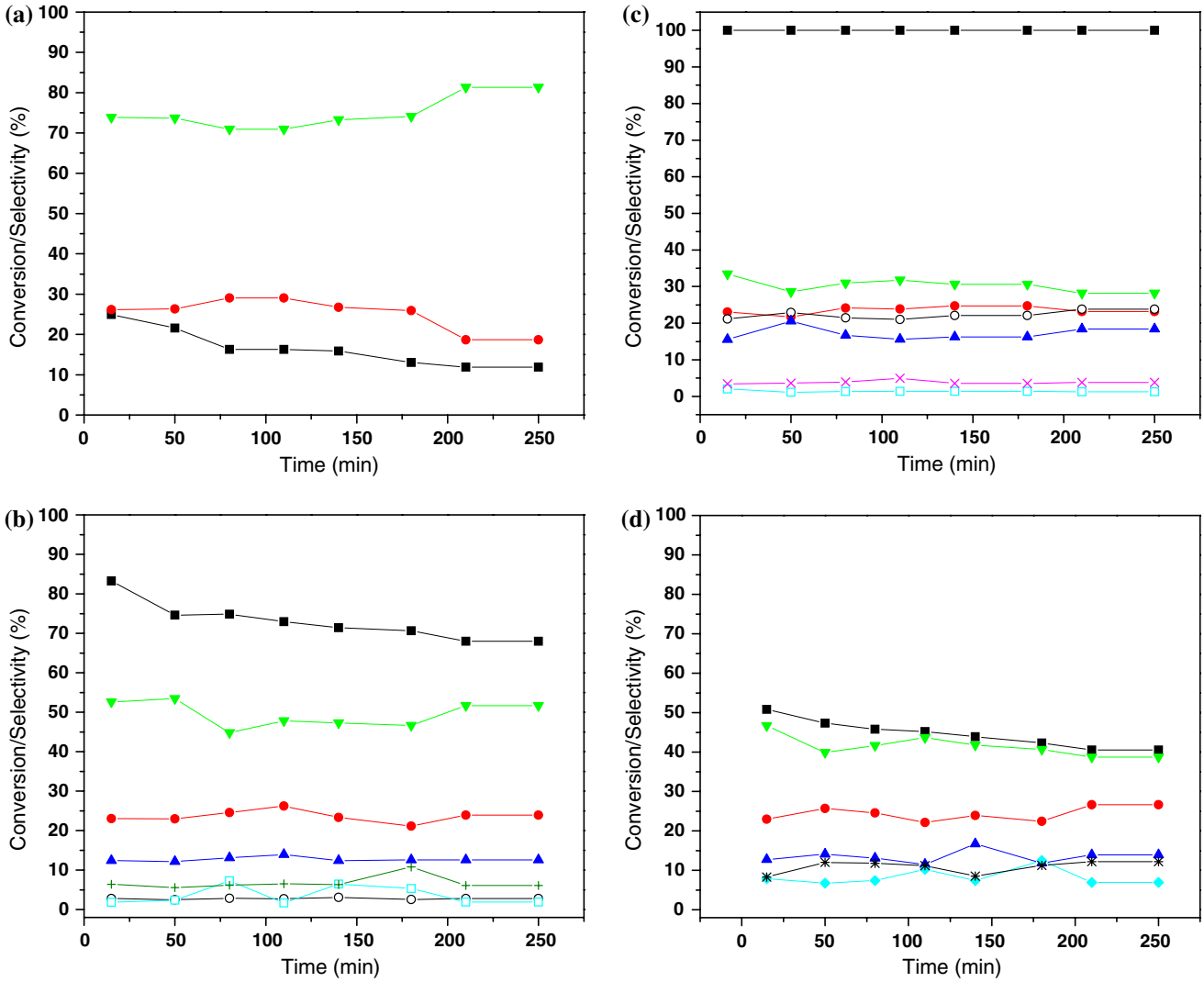

Fig. 4 Catalytic performance in the reforming of ethanol over: **a** $Gd_{0.2}Ce_{0.8}O_{2-x}$ nanorods at 400 °C, **b** $Gd_{0.2}Ce_{0.8}O_{2-x}$ nanorods at 500 °C, **c** $Gd_{0.2}Ce_{0.8}O_{2-x}$ nanorods at 600 °C and **d** commercial CeO_2 at 500 °C. Legends: ■ = C_2H_5OH conversion, ● = H_2, ○ = CH_4, ▲ = CO_2, ▼ = C_2H_4, □ = C_2H_6, + = CH_3CHO, * = CH_3COCH_3, × = CO, selectivities, respectively

promote hydrocarbon oxidation due to their redox properties [15–17]. The Boudouard reaction (Eq. 9) may contribute to the amount of CO_2 observed at this temperature, while the methanation reaction (Eq. 10) may contribute to the observed CH_4 concentration.

$$2CO \rightarrow C + CO_2 \quad (9)$$

$$CO + 3H_2 \rightarrow CH_4 + H_2O \quad (10)$$

It should be noted that the ethanol conversion over the commercial CeO_2 (Fig. 4d) was lower than that obtained over $Gd_{0.2}Ce_{0.8}O_{2-x}$ nanorods at 500 °C of reaction temperature. This is probably due to the low specific surface area of the commercial sample. Moreover, this particular catalyst was unique in that acetone was observed in the product stream. Therefore, the following reaction must have occurred over the commercial catalyst (Eq. 11):

$$2C_2H_5OH + H_2O \rightarrow 4H_2 + CO_2 + CH_3COCH_3 \quad (11)$$

Although the commercial CeO_2 catalyst also provides similar selectivity toward H_2 production, the major weaknesses of this catalyst is its natural low specific surface area resulting in low redox properties. Consequently, the lowest ethanol reforming reactivity was observed over this catalyst. Studies reported in the literature indicate that the enhancement of the redox properties of CeO_2 leads to an improvement in the reforming activity of cerium oxide-based catalysts, in addition, ceria nanorods can exhibit a greater capacity to

store oxygen than nanoparticles [18]. According to the results, the conversion of ethanol is affected by the morphologies of ceria-based catalysts. The poorer catalytic performance of the commercial CeO_2 could also be attributed to a smaller concentration of [110], [111] and [200] facets than in the case of $Gd_{0.2}Ce_{0.8}O_{2-x}$ nanorods. Previously, numerous studies have shown that in ceria nanoparticles the least reactive (111) planes are predominantly exposed [9]. The comparable reforming reactivities of the commercial CeO_2 and $Gd_{0.2}Ce_{0.8}O_{2-x}$ nanorods are in good agreement with results reported in the literature.

The relatively high selectivity toward ethylene achieved over the $Gd_{0.2}Ce_{0.8}O_{2-x}$ nanorods catalyst with low rates of deactivation can be considered a positive factor, since this hydrocarbon is a valuable product of the petrochemical industry.

Conclusions

In this study, we demonstrate that the use of microwave heating during hydrothermal treatment decreases the treatment time required to obtain gadolinium-doped ceria nanorods and that the oriented attachment is the dominant mechanism responsible for anisotropic growth. The nanorods synthesized showed better textural properties than the commercial CeO_2 and this reflected in the catalytic behaviors observed. It is worth emphasizing the complete conversion of ethanol and the stability of the $Gd_{0.2}Ce_{0.8}O_{2-x}$ nanorods catalyst at 600 °C, during 4 h of reaction. These are important factors in terms of achieving the economic viability of the ethanol reforming process. We believe that by supporting the $Gd_{0.2}Ce_{0.8}O_{2-x}$ nanorods with an active metal phase, such as nickel, this catalyst could provide excellent hydrogen selectivity with a high resistance toward carbon deposition. This point will be the subject of future publication.

Acknowledgements Financial support by FAPESP, FINEP and CNPq is gratefully acknowledged.

References

1. Kugai J, Velu S, Song C (2005) Catal Lett 101:255
2. Laosiripojana N, Sutthisripok W, Assabumrungrat S (2007) Chem Eng J 127:31
3. Al-Madfaa HA, Khader MM (2004) Mater Chem Phys 86:180
4. Godinho MJ, Gonçalves RF, Santos LPS, Varela JA, Longo E, Leite ER (2007) Mater Lett 61:1904
5. Wang S, Gu F, Li C, Cao H (2007) J Cryst Growth 307:386
6. Jiguang LI, Ikegami T, Wang Y, Mori T (2003) J Am Ceram Soc 86:915
7. Wang S, Maeda K (2002) J Am Ceram Soc 85:1750
8. Kaneko K, Inoke K, Freitag B, Hungria AB, Midgley PA, Hansen TW, Zhang J, Ohara S, Adschiri T (2007) Nano Lett 7:421
9. Zhou K, Wang X, Sun X, Peng Q, Li Y (2005) J Catal 229:206–212
10. Mai HX, Sun LD, Zhang YW, Si R, Feng W, Zhang HP, Liu HC, Yan CH (2005) J Phys Chem B 109:24380
11. Chen G, Li S, Jiao F, Yuan Q (2007) Catal Today 125:111
12. Varisli D, Dogu T, Dogu G (2007) Chem Eng Sci 62:5349
13. Sahaym U, Grant-Norton M (2008) J Mater Sci 43:5395. doi: 10.1007/s10853-008-2749-0
14. Godinho M, Ribeiro C, Longo E, Leite ER (2008) Cryst Growth Des 8:384
15. Idriss H (2004) Platinum Metals Rev 48:105
16. Pourfayaz F, Mortazavi Y, Khodadadi A, Ajami S (2008) Sens Actuators B 130:625
17. Fajardo HV, Probst LFD, Carreño NLV, Garcia ITS, Valentini A (2007) Catal Lett 119:228
18. Hsiao W, Lin YS, Chen YC, Lee CS (2007) Chem Phys Lett 441:294